

Published in final edited form as:

*Hepatology*. 2010 August ; 52(2): 678–690. doi:10.1002/hep.23721.

## Transgenic Expression of Cholesterol 7 $\alpha$ -Hydroxylase in the Liver Prevents High-Fat Diet–Induced Obesity and Insulin Resistance in Mice

Tiangang Li<sup>1</sup>, Erika Owsley<sup>1</sup>, Michelle Matozel<sup>1</sup>, Peter Hsu<sup>1</sup>, Colleen M. Novak<sup>2</sup>, and John Y. L. Chiang<sup>1</sup>

<sup>1</sup>Department of Integrative Medical Sciences, Northeastern Ohio Universities' Colleges of Medicine and Pharmacy, Rootstown, OH

<sup>2</sup>Department of Biological Sciences, Kent State University, Kent, OH

### Abstract

Cholesterol 7 $\alpha$ -hydroxylase (CYP7A1) is the rate-limiting enzyme in the bile acid biosynthetic pathway that converts cholesterol into bile acids in the liver. Recent studies have shown that bile acids may play an important role in maintaining lipid, glucose, and energy homeostasis. However, the role of CYP7A1 in the development of obesity and diabetes is currently unclear. In this study, we demonstrated that transgenic mice overexpressing Cyp7a1 in the liver [i.e., Cyp7a1 transgenic (Cyp7a1-tg) mice] were resistant to high-fat diet (HFD)–induced obesity, fatty liver, and insulin resistance. Cyp7a1-tg mice showed increased hepatic cholesterol catabolism and an increased bile acid pool. Cyp7a1-tg mice had increased secretion of hepatic very low density lipoprotein but maintained plasma triglyceride homeostasis. Gene expression analysis showed that the hepatic messenger RNA expression levels of several critical lipogenic and gluconeogenic genes were significantly decreased in HFD-fed Cyp7a1-tg mice. HFD-fed Cyp7a1-tg mice had increased whole body energy expenditure and induction of fatty acid oxidation genes in the brown adipose tissue.

**Conclusion**—This study shows that Cyp7a1 plays a critical role in maintaining whole body lipid, glucose, and energy homeostasis. The induction of CYP7A1 expression with the expansion of the hydrophobic bile acid pool may be a potential therapeutic strategy for treating metabolic disorders such as fatty liver diseases, obesity, and diabetes in humans.

Obesity and diabetes are closely associated with impaired lipid and glucose homeostasis, which significantly increases the risk of coronary heart disease.<sup>1</sup> Obesity often results from a Western lifestyle with overnutrition and a lack of exercise. Visceral fat accumulation due to increased caloric intake is known to cause organ insulin resistance.<sup>2</sup> It is believed that insulin resistance and overnutrition directly contribute to abnormal adiposity and hepatic very low density lipoprotein (VLDL) synthesis and thus lead to nonalcoholic fatty liver disease and dyslipidemia.<sup>3</sup>

Cholesterol 7 $\alpha$ -hydroxylase (CYP7A1) catalyzes the first and rate-limiting step in the bile acid biosynthetic pathway that converts cholesterol into bile acids and plays an important

---

Copyright © 2010 by the American Association for the Study of Liver Diseases.

Address reprint requests to: John Y. L. Chiang, Department of Integrative Medical Sciences, Northeastern Ohio Universities' Colleges of Medicine and Pharmacy, 4209 State Route 44, Rootstown, OH 44272. jchiang@neuoucom.edu; fax: 330-325-5910.

Potential conflict of interest: Nothing to report.

Additional Supporting Information may be found in the online version of this article.

role in regulating cholesterol and bile acid homeostasis. The role of CYP7A1 in regulating cholesterol homeostasis has been well established. Patients with mutations in the *CYP7A1* gene developed gallstones and premature atherosclerosis,<sup>4</sup> whereas Cyp7a1 transgenic (Cyp7a1-tg) mice were protected from atherogenic diet-induced atherosclerosis.<sup>5</sup> Bile acids are essential for the biliary secretion of cholesterol and phospholipids and the intestinal absorption of fats and nutrients. Bile acids also are versatile signaling molecules that activate nuclear receptors and cell signaling pathways, and they play critical roles in the regulation of lipid, glucose, and energy metabolism.<sup>6–8</sup> The critical role of bile acids in the regulation of triglyceride (TG) metabolism has been recognized for many years. The administration of a bile acid sequestrant or ileal resection depletes the bile acid pool and increases serum TG levels.<sup>9</sup> On the other hand, increasing the bile acid pool by the administration of chenodeoxycholic acid reduces plasma TGs.<sup>10</sup> Recent studies have revealed that bile acids may have a beneficial effect by improving obesity, insulin sensitivity, and whole body lipid and glucose homeostasis in mice.<sup>11, 12</sup> Bile acids may also negatively regulate serum TG levels by activating the nuclear receptor farnesoid X receptor (FXR), which induces small heterodimer partner (SHP) to inhibit sterol response element binding protein-1c (SREBP-1c) expression and its target genes in lipogenesis.<sup>11</sup> It has been reported that FXR represses hepatic expression of the gluconeogenic genes, phosphoenolpyruvate carboxykinase (PEPCK) and glucose-6-phosphatase (G6Pase), in the liver.<sup>13</sup> Activation of FXR significantly improved insulin sensitivity, hyperglycemia, and hyperlipidemia in db/db mice.<sup>12</sup> Bile acids also prevent diet-induced obesity in mice by activating the membrane bile acid receptor TGR5 to promote energy expenditure in brown adipocytes.<sup>14</sup>

In this study, we show that overexpression of CYP7A1 in the liver prevents high-fat diet (HFD)-induced obesity, fatty liver, and insulin resistance in mice. These results underscore the importance of bile acid homeostasis in the regulation of whole body lipid, glucose, and energy homeostasis.

## Materials and Methods

### Animals

Cyp7a1-tg mice overexpressing rat Cyp7a1 complementary DNA under the control of an apolipoprotein E3 (ApoE3) hepatic control region were originally generated by Dr. Roger A. Davis (San Diego State University) with a C57BL/6JxSJ strain and were backcrossed into a C57BL/6J background for five generations in the original laboratory.<sup>15</sup> We obtained the Cyp7a1-tg mice from the Mutant Mouse Regional Resource Center at the University of California Davis [strain name: B6.Cg-Tg (APOECyp7a1) 1Rjd/Mmcd]. Mice were further bred with wild-type C57BL/6J mice (Jackson Laboratory, Bar Harbor, ME). Transgenic mice and wild-type littermates (between six and eight generations) with >90% C57BL6J background were used in this study. We determined that Cyp7a1-tg mice carry two copies of the Cyp7a1 transgene. Mice were maintained on a standard chow diet and water *ad libitum* and housed in a room with a 12-hour light (6 am to 6 pm)/12-hour dark (6 pm to 6 am) cycle. To induce obesity and insulin resistance phenotypes, female and male mice (20–24 weeks old) were fed a Western HFD (Harlan-Teklad 88137; 42% fat calories and 0.2% cholesterol) for 2 to 4 months. Food intake was determined for a 2-day period. All animal protocols were approved by the institutional animal care and use committee.

### Insulin Sensitivity

Glucose tolerance tests were performed with an intraperitoneal injection of D-glucose (Sigma) at a dose of 2 g/kg of body weight after an overnight (16-hour) fast. Insulin tolerance tests were performed with an intraperitoneal injection of insulin (humulin R, Ely

Lilly and Co.) at a dose of 0.5 U/kg of body weight after a 4-hour fast. Blood samples were collected via the tail vein, and glucose was determined with a OneTouch Ultra glucometer (Life-Scan, Mountain View, CA).

## Histology

Liver or adipose tissues from overnight fasted mice were fixed in 10% formalin and embedded in paraffin. Tissue sections were then subjected to hematoxylin and eosin (H&E) staining. Hepatic glycogen was detected by a standard periodic acid-Schiff (PAS) staining method. For hepatic lipid staining, frozen liver tissues were cryosectioned, briefly fixed in 10% formalin, and stained with Oil Red O.

## Quantification of Tissue and Plasma Lipids, Glycogen, and Insulin

Liver tissues were homogenized, and lipids were extracted in a mixture of chloroform and methanol (2:1), dried, and dissolved in 5% Triton X-100 in isopropanol. Cholesterol and TG were determined with cholesterol assay kits (Calbiochem, San Diego, CA) and a TG-SL assay kit (Genzyme Diagnostic, Framingham, MA), respectively. Free fatty acids were determined with a fatty acid kit (BioVision, Inc., Mountain View, CA). A fast protein liquid chromatography (FPLC) analysis of the serum lipoprotein distribution was performed by the Mouse Metabolic Phenotyping Center at the University of Cincinnati. Serum lipoproteins were separated on a Superose 6 column, and 0.5-mL fractions were collected for the analysis of cholesterol and TG with assay kits. Serum ketone bodies were assayed for  $\beta$ -hydroxybutyrate with an assay kit. Hepatic glycogen was extracted in H<sub>2</sub>O and determined with a glycogen assay kit (BioVision). Fasting plasma insulin was measured with a mouse insulin enzyme-linked immunosorbent assay kit (Crystal Chem, Inc., Downers Grove, IL).

## Quantification of Bile Acids

Bile acids in the liver, intestine (whole with its contents), gallbladder, and feces were extracted in 75% ethanol at 50° for 4 hours. Serum samples were used directly. Bile acids were determined with a bile acid assay kit (Genzyme Diagnostic). The bile acid pool was determined as the total amount of bile acids in the liver, intestine, and gallbladder.

## Hepatic VLDL Secretion Assay

Mice were fasted for 4 hours and intraperitoneally injected with tyloxapol (Sigma) at a dose of 500 mg/kg of body weight. Blood samples were collected via the tail vein, and plasma TG was determined with a TG-SL assay kit (Genzyme Diagnostic).

## RNA Isolation and Quantitative Real-Time Polymerase Chain Reaction (PCR)

Total RNA was isolated with TRI Reagent (Sigma). Reverse-transcription reactions and real-time PCR were performed. All primer/probe sets for real-time PCR were TaqMan gene expression assays (Applied Biosystems, Foster City, CA). Amplification of ubiquitin C was used as an internal control. Relative messenger RNA (mRNA) expression was quantified with the comparative cycle threshold (Ct) method and was expressed as  $2^{-\Delta\Delta Ct}$ .

## Indirect Calorimetry and Body Composition

Indirect calorimetry and body composition measurements were performed at the Mouse Metabolic Phenotyping Center at the University of Cincinnati. Mice were fed an HFD for 4 months; O<sub>2</sub> consumption and CO<sub>2</sub> production were determined in free-fed mice for a 24-hour period. The respiratory quotient (RQ) was calculated as  $V_{CO_2}/V_{O_2}$  (where  $V_{CO_2}$  is the volume of carbon dioxide and  $V_{O_2}$  is the volume of oxygen). Body compositions were determined by echo nuclear magnetic resonance.

## CYP7A1 Enzyme Activity Assay

Mouse liver microsomes were isolated for the analysis of CYP7A1 enzyme activity with a high-performance liquid chromatography–based method as described previously.<sup>16</sup>

## Statistical Analysis

Results are expressed as means and standard errors. Statistical analysis was performed with the Student *t* test.  $P < 0.05$  was considered statistically significant.

## Results

### Cyp7a1-tg Mice Had an Increased Bile Acid Pool Size but Maintained Lipid Homeostasis

Cyp7a1-tg mice expressed 3-fold higher Cyp7a1 protein activity (Table 1 and Supporting Fig. 1A) and 2-fold higher enzyme activity in liver microsomes versus wild-type mice (Supporting Fig. 1B). When fed a chow diet, Cyp7a1-tg mice appeared normal and had a body weight similar to that of their wild-type littermates (Supporting Table 1). Cyp7a1-tg mice showed elevated plasma bile acid concentrations and bile acid contents in the gallbladder and the intestine. The bile acid pool size was increased by approximately 2.5-fold in Cyp7a1-tg mice. Interestingly, the hepatic bile acid concentration was not significantly different in Cyp7a1-tg mice and wild-type littermates, and this suggested the ability of the liver to maintain hepatic bile acid homeostasis. When fed a chow diet, Cyp7a1-tg mice generally maintained lipid homeostasis and showed normal hepatic and plasma TG and FFA levels. Plasma cholesterol levels were lower in Cyp7a1-tg mice than in wild-type controls. These results are consistent with the previous report.<sup>15</sup>

### Cyp7a1-tg Mice Were Resistant to Diet-Induced Weight Gain and Fatty Liver

To explore if Cyp7a1 may play a role in fat metabolism and glucose homeostasis, we fed female mice an HFD for 4 months and male mice an HFD for 2 months because wild-type male mice gained weight more quickly than female mice and became obese after 2 months of HFD feeding. Results for female mice are presented in the main text, and those for male mice are presented as supporting data. Although an HFD led to more weight gain in wild-type mice than a chow diet did, both male and female Cyp7a1-tg mice were resistant to HFD-induced weight gain (Fig. 1 A,B and Supporting Fig. 2A,B). Cyp7a1-tg mice fed an HFD had lower body fat mass and higher lean mass than wild-type mice (Fig. 1C). The difference in weight gain correlated well with the visceral fat mass and adipocyte size (Fig. 1D,E and Supporting Fig. 2C) in Cyp7a1-tg mice fed an HFD. The daily food intake (Fig. 1F) was similar between wild-type and Cyp7a1-tg mice and therefore was unlikely to contribute to the decreased weight gain in Cyp7a1-tg mice.

An analysis of the liver morphology revealed that the livers of HFD-fed wild-type mice were larger and pale, and this suggested increased lipid accumulation (Fig. 2A and Supporting Fig. 3A). In contrast, livers from HFD-fed Cyp7a1-tg mice appeared normal and had a reddish color. H&E staining of liver sections showed that livers of HFD-fed wild-type mice had unstained lipid inclusions, which were absent in the livers of HFD-fed Cyp7a1-tg mice (Fig. 2B). Oil Red O staining of lipids further confirmed a massive accumulation of neutral lipids in the livers of HFD-fed wild-type mice but not in the livers of Cyp7a1-tg mice (Fig. 2B). Hepatic cholesterol and TG contents were significantly higher in HFD-fed wild-type mice, whereas Cyp7a1-tg mice were completely resistant to HFD-induced hepatic lipid accumulation (Fig. 2 C,D). Serum alkaline phosphatase levels showed a tendency to decrease, but this did not reach statistical significance (Fig. 2E).

## Hepatic mRNA Expression in Cyp7a1-tg Mice

An analysis of hepatic gene expression (Table 1) revealed that in the chow-fed group, Cyp7a1-tg mice showed increased SREBP-1 and SREBP-2 mRNA expression versus wild-type mice. This was likely a result of increased cholesterol catabolism and relative cholesterol deprivation in the Cyp7a1-tg mouse livers. Interestingly, HFD feeding markedly induced mRNA expression of SREBP-1 and its target gene stearoyl-coenzyme A desaturase 1 in wild-type mice but not in Cyp7a1-tg mice. Fatty acid synthase (FAS) mRNA expression was higher in Cyp7a1-tg mice than in wild-type mice in both the chow and HFD groups and did not correlate with hepatic SREBP-1 levels. FAS is an FXR target gene<sup>17</sup>; thus, induction of FAS in Cyp7a1-tg mice could be due to bile acid activation of FXR in the liver. HFD feeding induced the mRNA expression of the hepatic fatty acid uptake transporter CD36 in wild-type mice but not in Cyp7a1-tg mice. This expression profile suggests that decreased hepatic lipogenesis and fatty acid uptake could alleviate HFD-induced hepatic fat accumulation. Expression of Cyp8b1, which is involved in synthesis of cholic acid was markedly inhibited. This explains the increased CDCA and hydrophobicity of bile acid pool in Cyp7a1-tg mice.<sup>15</sup> SHP expression was significantly induced by HFD in both wild type and Cyp7a1-tg mice. The mRNA levels of the proinflammatory cytokines tumor necrosis factor  $\alpha$ , interleukin-6, and transforming growth factor  $\beta$ 1 were significantly lower in HFD-fed Cyp7a1-tg mice. Because of increased SREBP-2 expression, hepatic 3-hydroxy-3-methyl-glutaryl-coenzyme A reductase and low-density lipoprotein (LDL) receptor expression was significantly higher in Cyp7a1-tg mice, and this suggested compensatory induction of cholesterol synthesis and LDL cholesterol uptake to maintain hepatic cholesterol homeostasis.

## Cyp7a1-tg Mice Had Higher Hepatic VLDL Secretion but Maintained Plasma Lipid Homeostasis

Obesity and fatty liver are often associated with increased hepatic VLDL production and hypertriglyceridemia. Surprisingly, despite lower hepatic TG contents, both male and female Cyp7a1-tg mice showed a higher rate of VLDL secretion in postprandial states (Fig. 3A and Supporting Fig. 4A). The mRNA and protein expression of microsomal triglyceride transport protein (MTP), which encodes the rate-limiting enzyme in the VLDL assembly, was significantly higher in the livers of Cyp7a1-tg mice versus wild-type mice (Fig. 3B,C), and this suggested an increased VLDL assembly rate. Analysis of plasma lipid levels showed that fasting plasma TG was not elevated in HFD-fed wild-type mice versus chow-fed controls (Fig. 3D), and this was consistent with the resistance of C57BL/6J mice to HFD-induced hypertriglyceridemia.<sup>11</sup> Interestingly, despite the increased hepatic VLDL secretion, Cyp7a1-tg mice did not show elevated fasting plasma TG levels (Fig. 3D and Supporting Fig. 4B), and this possibly suggested increased TG clearance in peripheral tissues. The fasting plasma FFA level was elevated in HFD-fed wildtype mice versus chow-fed controls and was significantly lower in HFD-fed Cyp7a1-tg mice (Fig. 3E); this was consistent with decreased adiposity. Serum cholesterol levels were significantly lower in Cyp7a1-tg mice in both chow-fed and HFD-fed groups (Fig. 3F and Supporting Fig. 4C). The fasting serum ketone body contents for Cyp7a1-tg male ( $2.18 \pm 0.2$  mg/dL) and female mice ( $3.10 \pm 0.42$  mg/dL) were significantly lower than those for wild-type male ( $4.57 \pm 0.70$  mg/dL) and female mice ( $5.68 \pm 0.46$  mg/dL); this was consistent with lower fasting serum FFA levels in Cyp7a1-tg mice versus wild-type mice. An FPLC analysis of serum lipoprotein profiles showed that HFD-fed wild-type mice had markedly increased concentrations of LDL cholesterol and LDL/high-density lipoprotein 1 (HDL1) particles (a shoulder in the size range between LDL and HDL), whereas the lipoprotein profiles of HFD-fed Cyp7a1-tg mice predominantly showed HDL cholesterol (Fig. 4A). Male wildtype and Cyp7a1-tg mice had increased VLDL cholesterol. Increased levels of LDL/HDL1 particles have been observed in ob/ob and db/db mice and in obese mice lacking ApoA-1<sup>18-20</sup>



because of a defect in HDL uptake and recycling in ob/ob mice.<sup>19</sup> Both male and female Cyp7a1-tg mice had increased TG contents in the VLDL particles (Fig. 4B). This was consistent with increased VLDL secretion in HFD-fed Cyp7a1-tg mice. In summary, Cyp7a1-tg mice had increased hepatic VLDL secretion despite lower hepatic fat contents, and this indicated that increased hepatic VLDL secretion in Cyp7a1-tg mice may have contributed to decreased hepatic fat accumulation.

### Cyp7a1-tg Mice Had Improved Glucose Homeostasis and Insulin Sensitivity

Wild-type mice fed an HFD had significantly elevated fasting glucose and insulin levels in comparison with chow-fed mice, and this was suggestive of impaired insulin sensitivity (Fig. 5A,B). These values in HFD-fed Cyp7a1-tg mice were comparable to those in chow-fed mice (Fig. 5A,B). Increased insulin sensitivity in Cyp7a1-tg mice was further confirmed by glucose tolerance testing (Fig. 5C and Supporting Fig. 5A) and insulin tolerance testing (Fig. 5D and Supporting Fig. 5B). The mRNA expression levels of the hepatic gluconeogenic gene G6Pase, but not PEPCK, were significantly lower in HFD-fed Cyp7a1-tg mice, and this indicated decreased fasting hepatic gluconeogenesis (Fig. 5E,F). These gene expression profiles reflected increased hepatic insulin sensitivity and were also consistent with the repressive effect of bile acids on gluconeogenic genes.<sup>13</sup> The absence of inhibition of PEPCK in Cyp7a1-tg mice could be due to an FXR response element in the PEPCK promoter that counteracts the negative regulation of PEPCK by SHP and insulin signaling.<sup>12</sup> The hepatic glycogen content was lower in HFD-fed mice versus chow-fed wild-type mice. In contrast, the liver glycogen contents in HFD-fed Cyp7a1-tg mice and chow-fed mice were similar (Fig. 6A). These observations were further confirmed by PAS staining of liver sections from these mice (Fig. 6B). Insulin is known to stimulate hepatic glycogen synthesis by phosphorylation (inactivation) of glycogen synthase kinase 3 $\beta$  (GSK3 $\beta$ ). Increased phosphorylation of AKT-1 and GSK3 $\beta$  is consistent with improved hepatic insulin signaling in the livers of Cyp7a1-tg mice (Fig. 6C,D). In summary, all results demonstrated that hepatic expression of Cyp7a1 improved glucose homeostasis and insulin sensitivity in HFD-fed Cyp7a1-tg mice.

### Cyp7a1-tg Mice Had Increased Energy Expenditure

The resistance to HFD-induced obesity may be one of the major mechanisms by which Cyp7a1-tg mice had improved overall lipid and glucose homeostasis and insulin sensitivity. To explore why HFD-fed Cyp7a1-tg mice had fewer adipocytes than HFD-fed wild-type mice despite significantly elevated hepatic VLDL production, we determined the energy expenditure in HFD-fed wild-type and Cyp7a1-tg mice by indirect calorimetry. HFD-fed Cyp7a1-tg mice had consistently higher O<sub>2</sub> consumption and CO<sub>2</sub> production than wild-type mice (Fig. 7A and Supporting Fig. 6). A lower RQ value ( $RQ = V_{CO_2}/V_{O_2}$ ) indicates higher utilization of fat as an energy source, whereas a higher RQ value indicates higher carbohydrate utilization. Dietary fat is known to have a glucose-sparing effect leading to a decreased RQ value. The increased RQ value in Cyp7a1-tg mice could be a result of less tissue fat available for oxidation in these mice or a result of improved insulin sensitivity that promotes tissue carbohydrate utilization. Bile acid-activated TGR5 signaling in brown adipose tissue (BAT) stimulated energy expenditure and decreased adiposity in HFD-fed mice.<sup>14</sup>

### CYP7A1-tg Mice Had Increased Expression of Genes Involved in Energy Metabolism

The HFD-fed wild-type mice had more BAT than Cyp7a1-tg mice (Fig. 7B, left panel). However, with normalization to body weight, the Cyp7a1-tg mice and wildtype mice had similar ratios of BAT to body weight (Fig. 7B, right panel). In BAT, uncoupling protein-1 (UCP-1) was induced in HFD-fed Cyp7a1-tg mice in comparison with HFD-fed wild-type mice (Fig. 7C, left panel). UCP-1 is the major uncoupling protein that is highly expressed in

BAT. Induction of UCP-1 uncouples mitochondrial oxidative phosphorylation to dissipate ATP energy as heat and reduces adiposity and body weight.<sup>21</sup> The mRNA expression levels of TGR5 were increased approximately 4-fold in BAT of Cyp7a1-tg mice (Fig. 7C, left panel). Expression levels of peroxisome proliferator-activated receptor  $\gamma$  coactivator-1 $\alpha$  and type 2 deiodinase mRNA were also significantly induced in BAT of Cyp7a1-tg mice (Fig. 7C, left panel). This gene expression profile in the BAT of Cyp7a1-tg mice was similar to that in the BAT of cholic acid-fed mice and HFD-fed mice,<sup>14</sup> and this supported the conclusion that bile acid-activated TGR5 signaling increased energy expenditure in BAT. In contrast, the mRNA expression levels of fatty acid oxidation genes were largely unchanged in the muscle of Cyp7a1-tg mice (Fig. 7C, right panel).

## Discussion

The potential role of the hepatic Cyp7a1 gene in preventing the development of obesity and diabetes has not been investigated previously. This study showed that increased hepatic CYP7A1 expression improved several parameters of metabolic syndrome, including obesity, hepatic steatosis, and insulin resistance, in mice. Resistance of Cyp7a1-tg mice to HFD-induced obesity, insulin resistance, and hyperlipidemia could be a result of both enhanced hepatic CYP7A1 enzyme activity and activation of cellular bile acid signaling due to an expanded bile acid pool. These findings underscore the importance of bile acid homeostasis in maintaining whole body lipid, glucose, and energy homeostasis.

In the liver, free fatty acids (FFAs) taken up from circulation are esterified into TGs and assembled into VLDL particles, which are secreted and transported to adipocytes for storage. Increased adipose mass due to excessive caloric intake is known to account for many manifestations of metabolic syndrome. Elevated cytokine production from adipose tissue is associated with insulin resistance.<sup>22</sup> Abnormal adipose lipolysis due to the combined effect of increased adiposity and insulin resistance may lead to increased transport of free fatty acids to the liver and other peripheral tissues. This may not only cause impaired glucose utilization and organ insulin resistance but also contribute significantly to the development of nonalcoholic fatty liver disease. Thus, resistance to HFD-induced obesity and visceral fat accumulation may be one of the major mechanisms by which Cyp7a1-tg mice had improved overall lipid and glucose homeostasis and insulin sensitivity. Increased hepatic VLDL secretion and normal fasting serum TG levels in Cyp7a1-tg mice also suggest that fat clearance or fat metabolism in peripheral tissues may be increased to account for decreased adiposity. Indeed, the indirect calorimetry measurements and mRNA expression profile supported increased energy expenditure in BAT of Cyp7a1-tg mice. The role of BAT in preventing obesity in Cyp7a1-tg mice could be further supported by previous studies showing that expansion of the bile acid pool by cholic acid feeding activated TGR5 signaling in BAT and prevented HFD-induced obesity in mice.<sup>14</sup> Transgenic expression of UCP-1 in BAT increases energy expenditure, reduces adiposity, and prevents obesity in mice.<sup>23, 24</sup> BAT is also present in adult humans and is inversely correlated with obesity.<sup>25</sup> In contrast, bile acid sequestrants, which block intestine bile acid absorption, reduce the bile acid pool size, and induce hepatic CYP7A1 expression, do not reduce body weight and prevent obesity.<sup>26, 27</sup> Thus, induction of CYP7A1 without expansion of the bile acid pool may not prevent obesity.

Although HFD feeding induced hepatic TG and cholesterol accumulation in wild-type mice, Cyp7a1-tg mice were protected from HFD-induced fatty liver. In addition to decreased adiposity, several hepatic mechanisms could account for the resistance of Cyp7a1-tg mice to hepatic steatosis. Lower SREBP-1 expression in HFD-fed Cyp7a1-tg mice suggests that repression of hepatic lipogenesis could contribute to decreased fat accumulation in HFD-fed Cyp7a1-tg mice. Bile acid activation of FXR has been shown to induce SHP to repress

SREBP-1 and its target genes in lipogenesis.<sup>11</sup> However, in chow-fed mice, SREBP-1 expression was significantly higher in Cyp7a1-tg mice despite a larger bile acid pool and induction of SHP, and this brings into question the relative importance of the FXR/SHP pathway in the repression of SREBP-1 in Cyp7a1-tg mice. Insulin is known to induce SREBP-1 and lipogenesis. Induction of SREBP-1 in HFD-fed wild-type mice was likely a result of hepatic insulin resistance and hyperinsulinemia. Decreased SREBP-1 expression in HFD-fed Cyp7a1-tg mice could be due to increased insulin sensitivity. Cyp7a1-tg mice showed a robust increase in hepatic VLDL secretion. Increased CYP7A1 activity may cause cholesterol deprivation in the liver and subsequent induction of SREBP-1 and lipogenesis, which promotes hepatic VLDL production in Cyp7a1-tg mice.<sup>15</sup> However, our results showed that when fed an HFD, Cyp7a1-tg mice still had increased hepatic VLDL secretion despite significantly lower SREBP-1 expression and fat content; this suggested that increased hepatic VLDL secretion in Cyp7a1-tg mice was not due to SREBP-1-dependent lipogenesis. Instead, hepatic MTP mRNA expression was increased in Cyp7a1-tg mice, and this suggested that the increased VLDL secretion could be due to increased VLDL assembly. Induction of CD36 in the liver causes hepatic TG accumulation and fatty liver disease.<sup>28</sup> HFD-fed Cyp7a1-tg mice had lower hepatic CD36 expression; together with lower plasma FFA levels, this could lead to reduced hepatic fatty acid uptake. Thus, decreased hepatic lipogenesis, increased hepatic VLDL secretion, and reduced hepatic fatty acid uptake could alleviate HFD-induced fatty liver in Cyp7a1-tg mice.

Cyp7a1-tg mice had improved insulin sensitivity, as reflected by glucose and insulin tolerance tests, and normal fasting glucose and insulin levels. Increased phosphorylation of AKT and GSK3 $\beta$  and increased glycogen content in the livers of Cyp7a1-tg mice were indicative of improved hepatic insulin sensitivity. Improved insulin sensitivity in Cyp7a1-tg mice was likely a result of both decreased adiposity and the absence of hepatic fat accumulation. Cyp7a1-tg mice showed an increased RQ value suggesting that Cyp7a1-tg mice had improved overall glucose utilization. Hepatic expression of G6Pase was decreased in Cyp7a1-tg mice fed an HFD, and this suggested decreased gluconeogenesis. On the one hand, repression of gluconeogenesis could be secondary to improved insulin signaling in the liver; on the other hand, bile acid activation of FXR has been shown to directly repress the expression of gluconeogenic genes. A recent study has reported that activation of TGR5 by bile acid derivatives promotes intestinal glucagonlike peptide 1 (GLP-1) release and improves insulin sensitivity in diabetic obese mice.<sup>29</sup> It is likely that Cyp7a1-tg mice may also have increased serum GLP-1, which stimulates insulin secretion and prevents insulin resistance and diabetes.

Recent studies have suggested that drugs targeting bile acid signaling may be beneficial for the treatment of metabolic disorders.<sup>7</sup> FXR agonists have been shown to improve hepatic lipid and glucose homeostasis in mice but have not been shown to regulate energy expenditure and adiposity. More recent studies have identified synthetic bile acid derivatives as selective TGR5 agonists that may have therapeutic potential for treating diabetes and obesity.<sup>8, 14</sup> According to this study, induction of hepatic CYP7A1 not only achieved a hypocholesterolemic effect but also prevented HFD-induced obesity, fatty liver, and insulin resistance. Induction of CYP7A1 expression with expansion of a hydrophobic bile acid pool may be a more promising treatment strategy for liver diseases and metabolic disorders. CYP7A1 mRNAs have very short half-lives of less than 30 minutes. It has been reported recently that apolipoprotein B100 editing enzyme complex-1 (Apobec-1) binds to the AU-rich sequences in the 3'-untranslated region (3'-UTR) of CYP7A1 mRNA and increases CYP7A1 mRNA and protein levels.<sup>30</sup> Gene transfer of Apobec-1 may stabilize CYP7A1 mRNAs and increase CYP7A1 protein and enzyme activity. We have identified a functional microRNA-122a binding site in the 3'-UTR of human CYP7A1 mRNA (Song et al. *J Lipid*



Res, 2010, in press.). MicroRNA-122a inhibitors (antagomirs) may be transferred into the liver to induce CYP7A1 enzyme and activity.

## Supplementary Material

Refer to Web version on PubMed Central for supplementary material.

## Acknowledgments

Supported by This study was supported by the National Institutes of Health (grants DK44442 and DK58379 to John Y. L. Chiang and grant NINDS55859 to Colleen M. Novak).

## Abbreviations

<b>ACC</b>	acetyl coenzyme A carboxylase
<b>ALT</b>	alanine aminotransferase
<b>APO</b>	apolipoprotein
<b>Apobec-1</b>	apolipoprotein B100 editing enzyme complex-1
<b>BAT</b>	brown adipose tissue
<b>BW</b>	body weight
<b>CPT1</b>	carnitine palmitoyltransferase 1
<b>Ct</b>	cycle threshold
<b>CYP7A1</b>	cholesterol 7 $\alpha$ -hydroxylase
<b>Cyp7a1-tg</b>	cholesterol 7 $\alpha$ -hydroxylase transgenic
<b>CYP8B1</b>	cholesterol 12 $\alpha$ -hydroxylase
<b>Dio2</b>	type 2 deiodinase
<b>FAS</b>	fatty acid synthase
<b>FFA</b>	free fatty acid
<b>FPLC</b>	fast protein liquid chromatography
<b>FXR</b>	farnesoid X receptor
<b>G6Pase</b>	glucose-6-phosphatase
<b>GLP-1</b>	glucagon-like peptide 1
<b>GSK3<math>\beta</math></b>	glycogen synthase kinase 3 $\beta$
<b>GTT</b>	glucose tolerance test
<b>H&amp;E</b>	hematoxylin and eosin
<b>HDL</b>	high-density lipoprotein
<b>HFD</b>	high-fat diet
<b>HMG-CoA</b>	3-hydroxy-3-methyl-glutaryl-coenzyme A
<b>IL6</b>	interleukin-6
<b>IP</b>	immunoprecipitation
<b>ITT</b>	insulin tolerance test

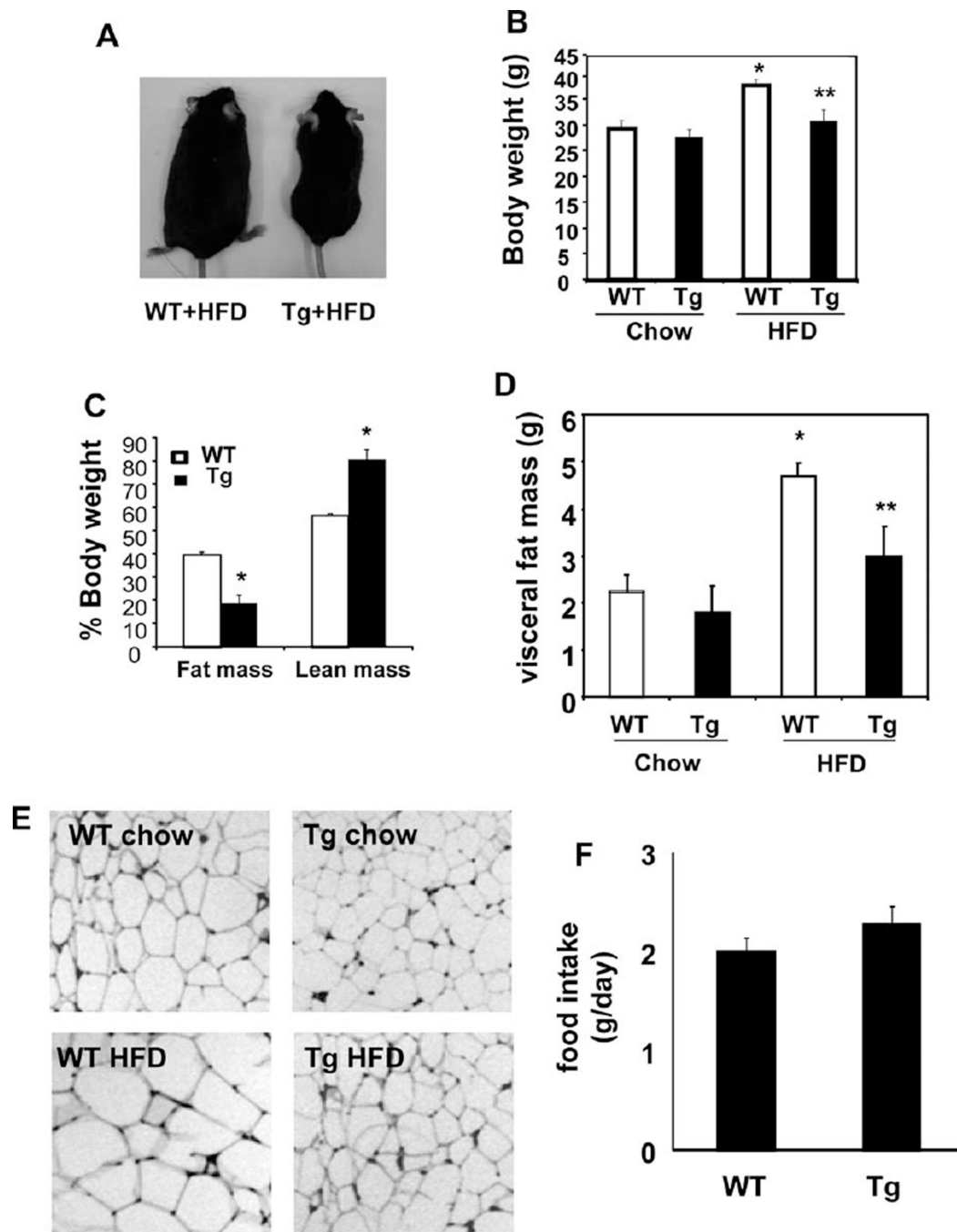
<b>LDL</b>	low-density lipoprotein
<b>LDLR</b>	low-density lipoprotein receptor
<b>mRNA</b>	messenger RNA
<b>MTP</b>	microsomal triglyceride transport protein
<b>ND</b>	not determined
<b>PAS</b>	periodic acid-Schiff
<b>PCR</b>	polymerase chain reaction
<b>PEPCK</b>	phosphoenolpyruvate carboxykinase
<b>PGC1<math>\alpha</math></b>	peroxisome proliferator-activated receptor $\gamma$ coactivator-1 $\alpha$
<b>PPAR<math>\alpha</math></b>	peroxisome proliferator-activated receptor $\alpha$
<b>RQ</b>	respiratory quotient
<b>SCD-1</b>	stearoyl-coenzyme A desaturase 1
<b>SHP</b>	small heterodimer partner
<b>SREBP</b>	sterol response element binding protein
<b>Tg</b>	transgenic
<b>TG</b>	triglyceride
<b>TGF<math>\beta</math>1</b>	transforming growth factor $\beta$ 1
<b>TNF<math>\alpha</math></b>	tumor necrosis factor $\alpha$
<b>UCP-1</b>	uncoupling protein-1
<b>UTR</b>	untranslated region
<b>V<sub>CO2</sub></b>	volume of carbon dioxide
<b>VLDL</b>	very low density lipoprotein
<b>V<sub>O2</sub></b>	volume of oxygen
<b>WT</b>	wild-type

## References

1. Schwartz SL. Diabetes and dyslipidaemia. *Diabetes Obes Metab.* 2006; 8:355–364. [PubMed: 16776742]
2. Biddinger SB, Kahn CR. From mice to men: insights into the insulin resistance syndromes. *Annu Rev Physiol.* 2006; 68:123–158. [PubMed: 16460269]
3. Farrell GC, Larter CZ. Nonalcoholic fatty liver disease: from steatosis to cirrhosis. *HEPATOLOGY.* 2006; 43:S99–S112. [PubMed: 16447287]
4. Pullinger CR, Eng C, Salen G, Shefer S, Batta AK, Erickson SK, et al. Human cholesterol 7 $\alpha$ -hydroxylase (CYP7A1) deficiency has a hypercholesterolemic phenotype. *J Clin Invest.* 2002; 110:109–117. [PubMed: 12093894]
5. Miyake JH, Duong-Polk XT, Taylor JM, Du EZ, Castellani LW, Lusic AJ, et al. Transgenic expression of cholesterol-7 $\alpha$ -hydroxylase prevents atherosclerosis in C57BL/6J mice. *Arterioscler Thromb Vasc Biol.* 2002; 22:121–126. [PubMed: 11788471]
6. Chiang JY. Bile acids: regulation of synthesis. *J Lipid Res.* 2009; 50:1955–1966. [PubMed: 19346330]

7. Lefebvre P, Cariou B, Lien F, Kuipers F, Staels B. Role of bile acids and bile acid receptors in metabolic regulation. *Physiol Rev*. 2009; 89:147–191. [PubMed: 19126757]
8. Thomas C, Pellicciari R, Pruzanski M, Auwerx J, Schoonjans K. Targeting bile-acid signalling for metabolic diseases. *Nat Rev Drug Discov*. 2008; 7:678–693. [PubMed: 18670431]
9. Grundy SM, Ahrens EH Jr, Salen G. Interruption of the enterohepatic circulation of bile acids in man: comparative effects of cholestyramine and ileal exclusion on cholesterol metabolism. *J Lab Clin Med*. 1971; 78:94–121. [PubMed: 5569253]
10. Angelin B, Einarsson K, Hellstrom K, Leijd B. Effects of cholestyramine and chenodeoxycholic acid on the metabolism of endogenous triglyceride in hyperlipoproteinemia. *J Lipid Res*. 1978; 19:1017–1024. [PubMed: 731123]
11. Watanabe M, Houten SM, Wang L, Moschetta A, Mangelsdorf DJ, Heyman RA, et al. Bile acids lower triglyceride levels via a pathway involving FXR, SHP, and SREBP-1c. *J Clin Invest*. 2004; 113:1408–1418. [PubMed: 15146238]
12. Zhang Y, Lee FY, Barrera G, Lee H, Vales C, Gonzalez FJ, et al. Activation of the nuclear receptor FXR improves hyperglycemia and hyperlipidemia in diabetic mice. *Proc Natl Acad Sci U S A*. 2006; 103:1006–1011. [PubMed: 16410358]
13. Yamagata K, Daitoku H, Shimamoto Y, Matsuzaki H, Hirota K, Ishida J, et al. Bile acids regulate gluconeogenic gene expression via small heterodimer partner-mediated repression of hepatocyte nuclear factor 4 and Foxo1. *J Biol Chem*. 2004; 279:23158–23165. [PubMed: 15047713]
14. Watanabe M, Houten SM, Matakai C, Christoffolete MA, Kim BW, Sato H, et al. Bile acids induce energy expenditure by promoting intracellular thyroid hormone activation. *Nature*. 2006; 439:484–489. [PubMed: 16400329]
15. Miyake JH, Doung XD, Strauss W, Moore GL, Castellani LW, Curtiss LK, et al. Increased production of apolipoprotein B-containing lipoproteins in the absence of hyperlipidemia in transgenic mice expressing cholesterol 7 $\alpha$ -hydroxylase. *J Biol Chem*. 2001; 276:23304–23311. [PubMed: 11323427]
16. Chiang JY. Reversed-phase high-performance liquid chromatography assay of cholesterol 7 $\alpha$ -hydroxylase. *Methods Enzymol*. 1991; 206:483–491. [PubMed: 1784233]
17. Matsukuma KE, Bennett MK, Huang J, Wang L, Gil G, Osborne TF. Coordinated control of bile acids and lipogenesis through FXR-dependent regulation of fatty acid synthase. *J Lipid Res*. 2006; 47:2754–2761. [PubMed: 16957179]
18. Silver DL, Jiang XC, Tall AR. Increased high density lipoprotein (HDL), defective hepatic catabolism of ApoA-I and ApoA-II, and decreased ApoA-I mRNA in ob/ob mice. Possible role of leptin in stimulation of HDL turnover. *J Biol Chem*. 1999; 274:4140–4146. [PubMed: 9933608]
19. Silver DL, Wang N, Tall AR. Defective HDL particle uptake in ob/ob hepatocytes causes decreased recycling, degradation, and selective lipid uptake. *J Clin Invest*. 2000; 105:151–159. [PubMed: 10642593]
20. Gruen ML, Plummer MR, Zhang W, Posey KA, Linton MF, Fazio S, et al. Persistence of high density lipoprotein particles in obese mice lacking apolipoprotein A-I. *J Lipid Res*. 2005; 46:2007–2014. [PubMed: 15995171]
21. Krauss S, Zhang CY, Lowell BB. The mitochondrial uncoupling-protein homologues. *Nat Rev Mol Cell Biol*. 2005; 6:248–261. [PubMed: 15738989]
22. Karalis KP, Giannogonas P, Kodela E, Koutmani Y, Zoumakis M, Teli T. Mechanisms of obesity and related pathology: linking immune responses to metabolic stress. *FEBS J*. 2009; 276:5747–5754. [PubMed: 19754872]
23. Rossmeisl M, Barbatelli G, Flachs P, Brauner P, Zingaretti MC, Marelli M, et al. Expression of the uncoupling protein 1 from the aP2 gene promoter stimulates mitochondrial biogenesis in unilocular adipocytes in vivo. *Eur J Biochem*. 2002; 269:19–28. [PubMed: 11784294]
24. Kopecky J, Clarke G, Enerback S, Spiegelman B, Kozak LP. Expression of the mitochondrial uncoupling protein gene from the aP2 gene promoter prevents genetic obesity. *J Clin Invest*. 1995; 96:2914–2923. [PubMed: 8675663]
25. Cypess AM, Lehman S, Williams G, Tal I, Rodman D, Goldfine AB, et al. Identification and importance of brown adipose tissue in adult humans. *N Engl J Med*. 2009; 360:1509–1517. [PubMed: 19357406]

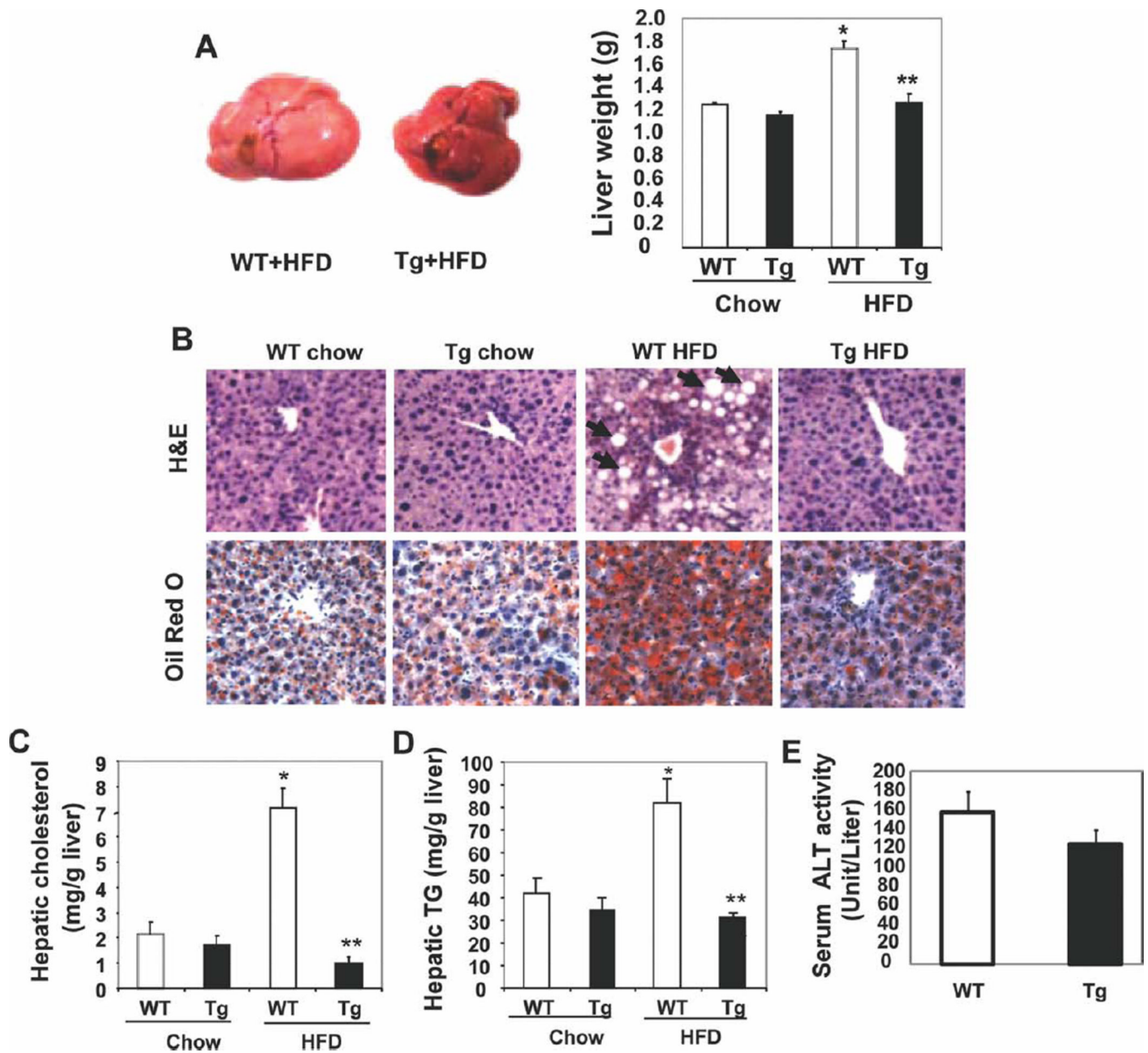
26. Goldberg RB, Fonseca VA, Truitt KE, Jones MR. Efficacy and safety of colesevelam in patients with type 2 diabetes mellitus and inadequate glycemic control receiving insulin-based therapy. *Arch Intern Med.* 2008; 168:1531–1540. [PubMed: 18663165]
27. Staels B. A review of bile acid sequestrants: potential mechanism(s) for glucose-lowering effects in type 2 diabetes mellitus. *Postgrad Med.* 2009; 121:25–30. [PubMed: 19494475]
28. Zhou J, Febbraio M, Wada T, Zhai Y, Kuruba R, He J, et al. Hepatic fatty acid transporter Cd36 is a common target of LXR, PXR, and PPARgamma in promoting steatosis. *Gastroenterology.* 2008; 134:556–567. [PubMed: 18242221]
29. Thomas C, Gioiello A, Noriega L, Strehle A, Oury J, Rizzo G, et al. TGR5-mediated bile acid sensing controls glucose homeostasis. *Cell Metab.* 2009; 10:167–177. [PubMed: 19723493]
30. Xie Y, Blanc V, Kerr TA, Kennedy S, Luo J, Newberry EP, et al. Decreased expression of cholesterol 7 $\alpha$ -hydroxylase and altered bile acid metabolism in apobec-1 $^{-/-}$  mice lead to increased gallstone susceptibility. *J Biol Chem.* 2009; 284:16860–16871. [PubMed: 19386592]



**Fig. 1.**

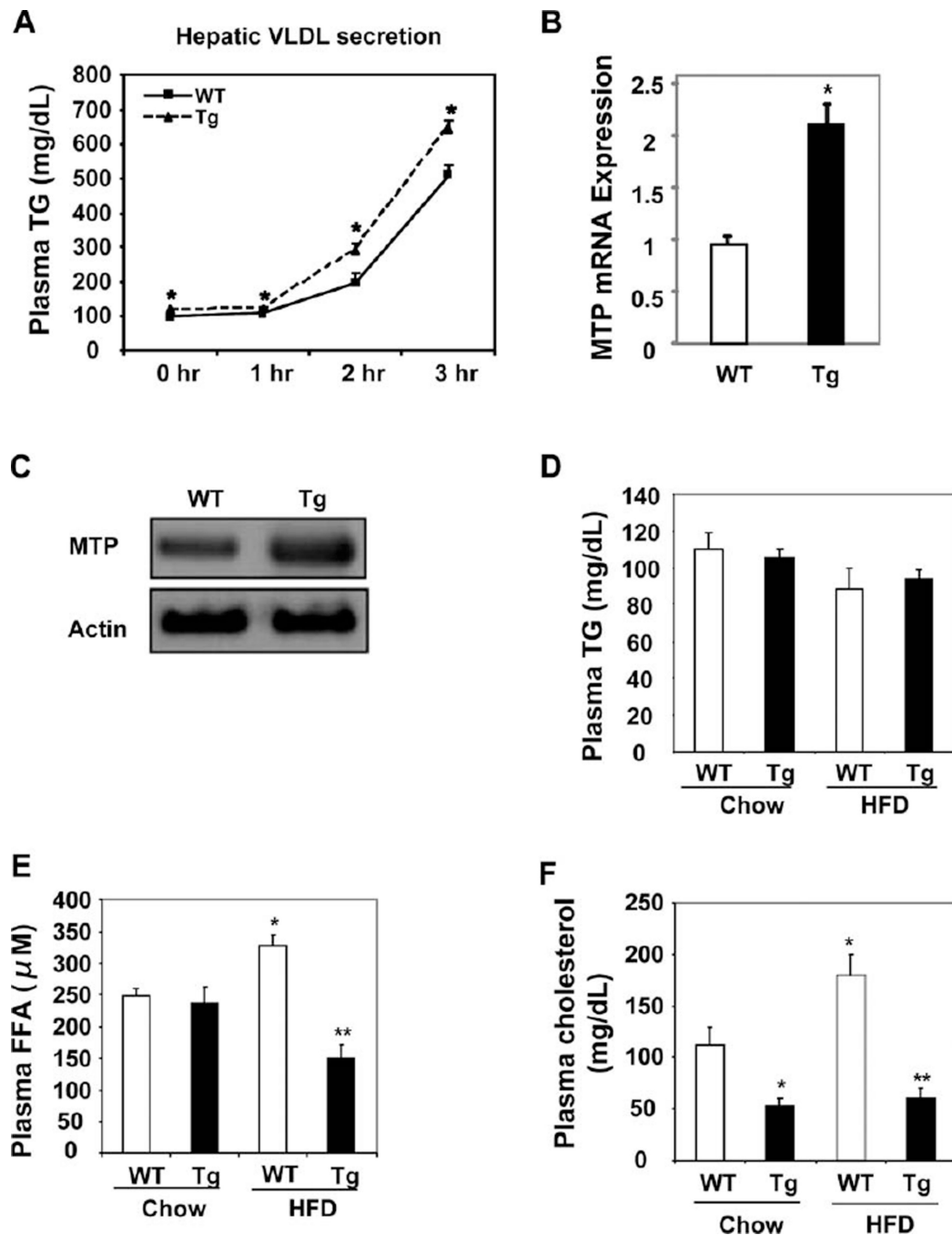
Tg expression of Cyp7a1 in the mouse liver prevented weight gain and reduced adiposity. Female WT or Cyp7a1-tg mice were fed either a chow diet or HFD for 4 months, and (A,B) the body weight, (C) body composition, (D) visceral fat mass, (E) H&E staining of adipocytes, and (F) food intake were determined. Results are expressed as means and standard errors (n =6–10). \*Statistically significant difference ( $P < 0.05$ ) versus WT mice on chow; \*\*statistically significant difference ( $P < 0.05$ ) versus WT mice on an HFD. Abbreviations: Tg, transgenic; WT, wild-type.





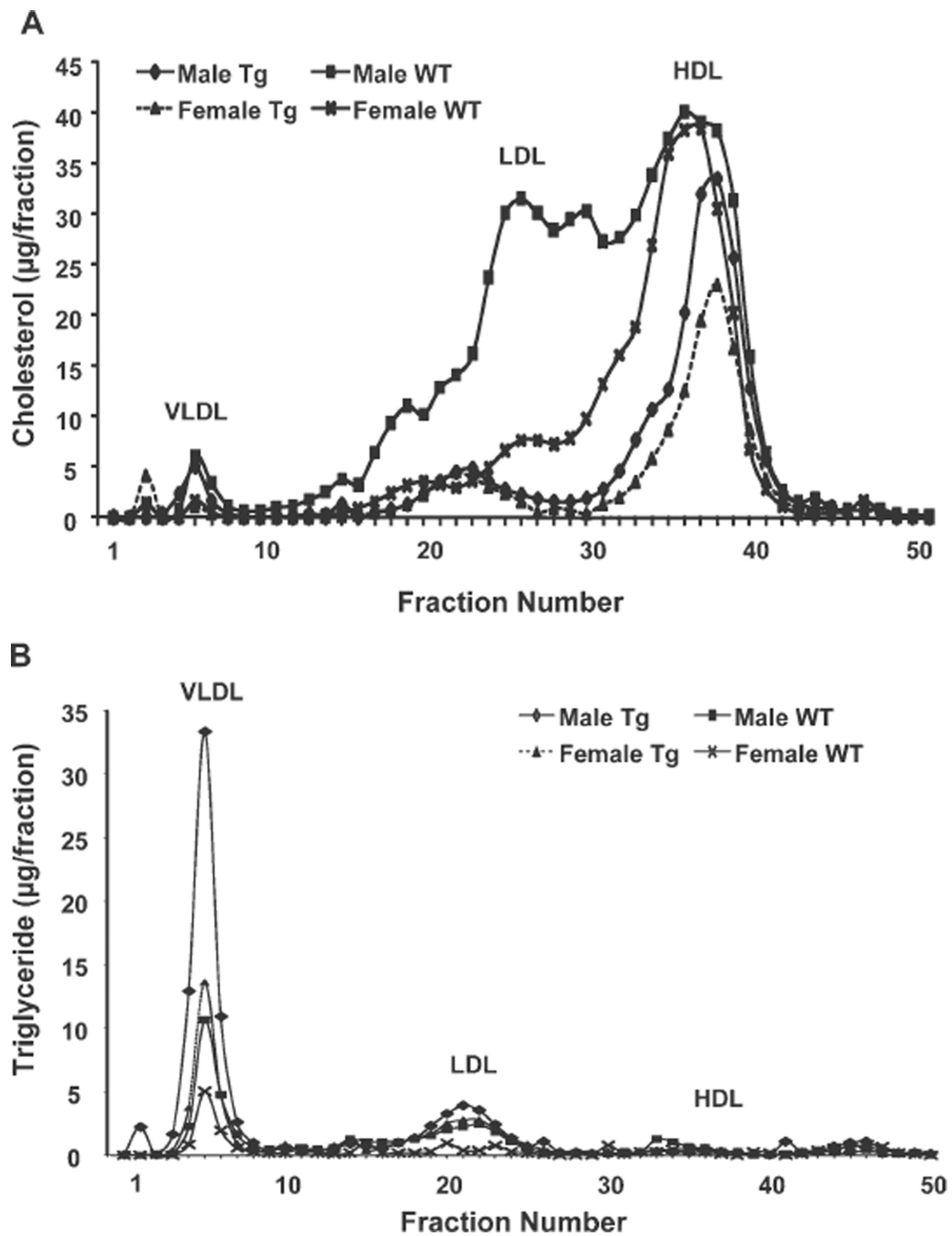
**Fig. 2.**

Tg expression of Cyp7a1 in the mouse liver prevented fatty liver. Female CYP7A1-tg mice were fed chow or an HFD for 4 months. Mice were fasted overnight. (A) The liver weight was determined. (B) H&E staining and Oil Red O staining of liver sections. Arrows indicate unstained lipid inclusions. (C,D) Hepatic cholesterol and TG contents. (E) Serum ALT levels in WT and CYP7A1-tg mice fed an HFD. Results are expressed as means and standard errors (n = 8–10). \*Statistically significant difference ( $P < 0.05$ ) versus chow-fed WT mice; \*\*statistically significant difference ( $P < 0.05$ ) versus HFD-fed WT mice. Abbreviations: ALT, alanine aminotransferase; Tg, transgenic; WT, wild-type.

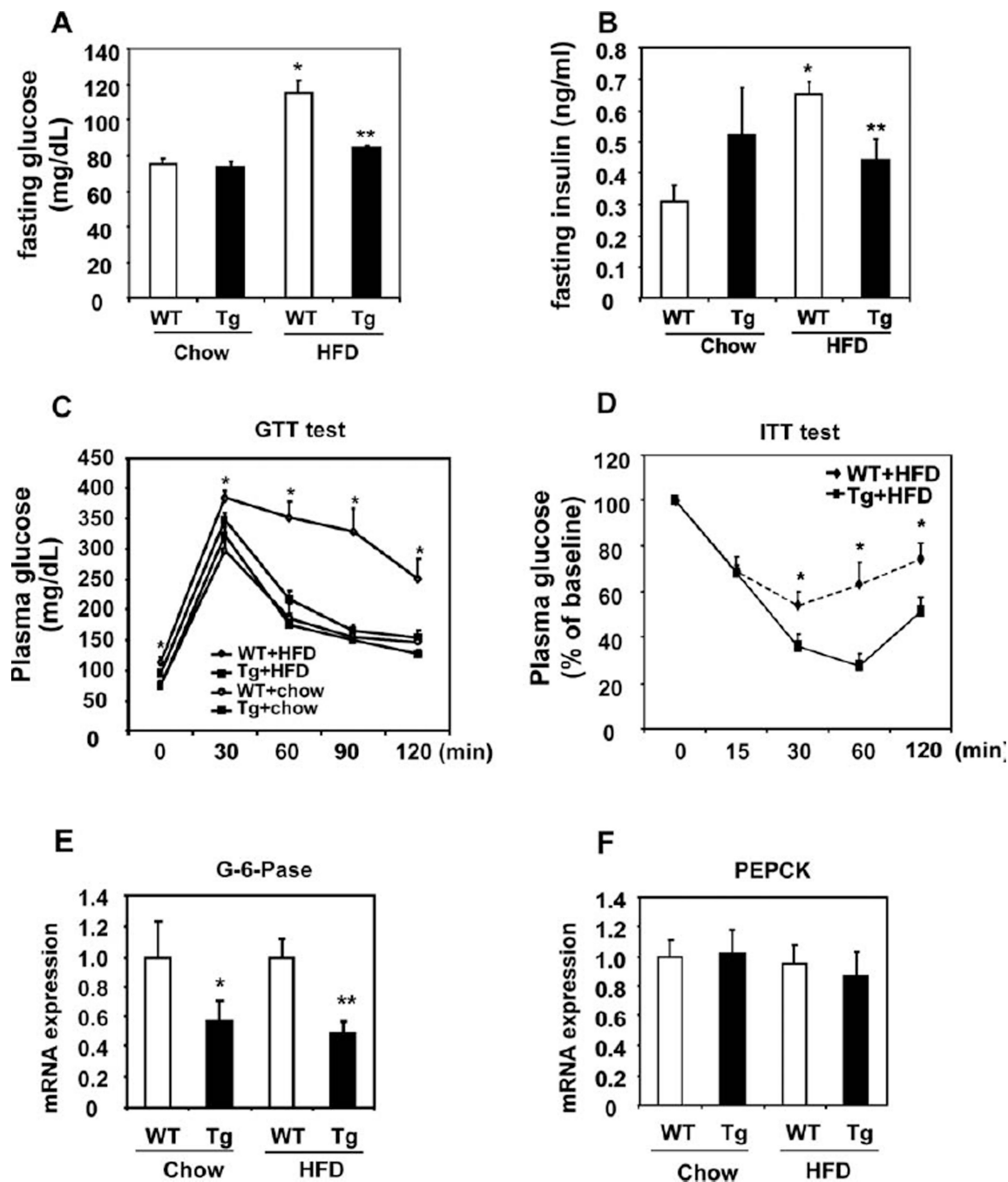


**Fig. 3.** Cyp7a1-tg mice showed increased hepatic VLDL secretion but maintained plasma TG homeostasis. Female mice were fed an HFD for 4 months. (A) Mice were briefly fasted for 4 hours, and the hepatic VLDL secretion was assayed after an intraperitoneal injection of taloxapol. (B,C) Hepatic mRNA and protein expression of MTP in mice fed for 4 hours after overnight fasting. Liver samples were pooled from six mice per group for western blot analysis of MTP protein. (D-F) Plasma cholesterol, TG, and FFA levels in mice fasted overnight. Results are expressed as means and standard errors (n = 6–8). \*Statistically significant difference ( $P < 0.05$ ) versus chow-fed WT mice; \*\*statistically significant

difference ( $P < 0.05$ ) versus HFD-fed WT mice. Abbreviations: Tg, transgenic; WT, wild-type.

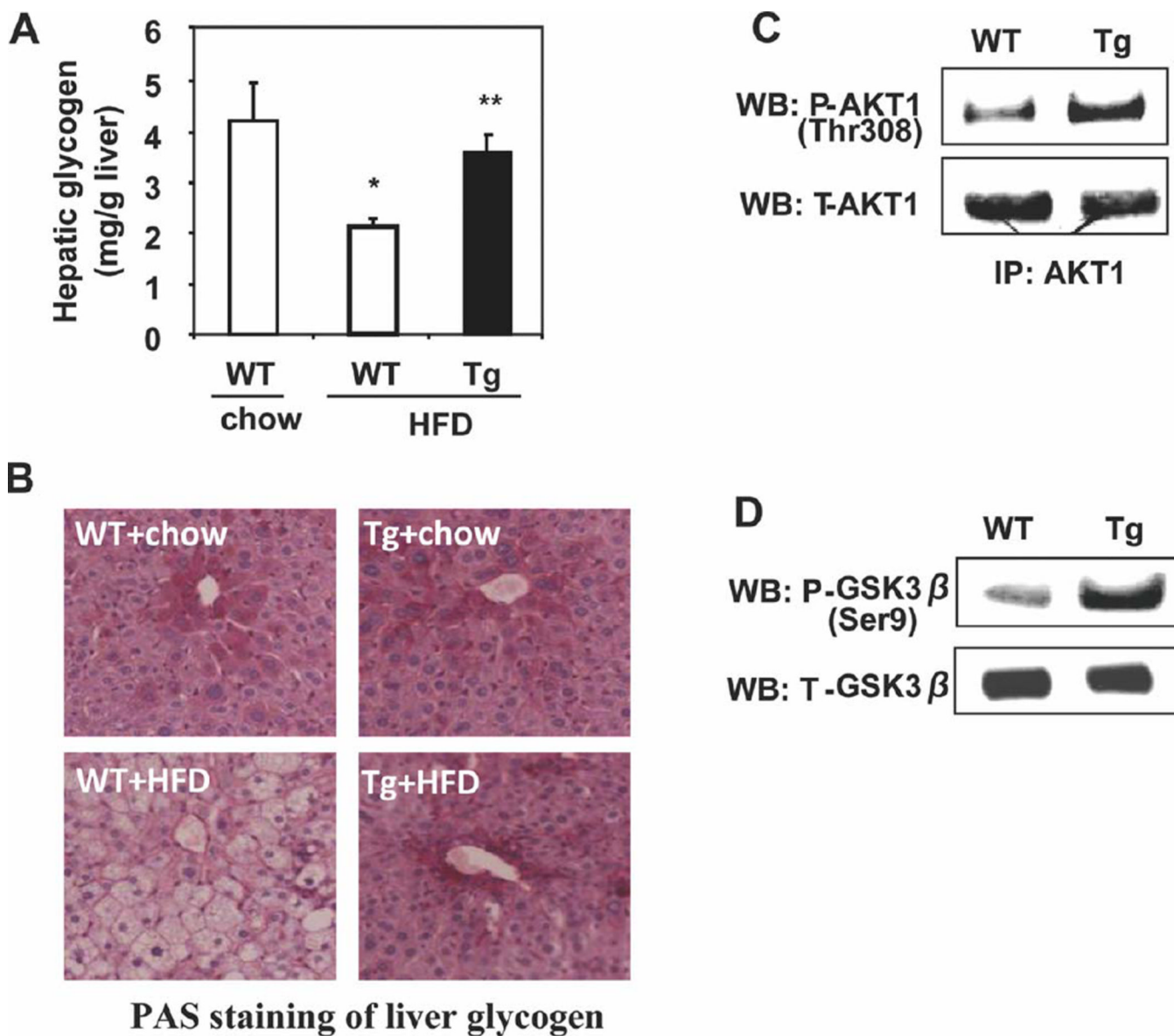


**Fig. 4.** FPLC analysis of the plasma lipoprotein profile for HFD-fed WT and Cyp7a1-tg male and female mice. Mice were fed an HFD for 4 month. After 6 hours of fasting, serum was collected and pooled (four mice per group). Serum lipoproteins were separated by FPLC with a Superose 6 column, and 0.5-mL fractions were collected for the analysis of (A) cholesterol and (B) TG contents in each by respective assay kits. Abbreviations: Tg, transgenic; WT, wild-type.



**Fig. 5.** Cyp7a1-tg mice showed improved insulin sensitivity and glucose homeostasis. Female mice were fed either a chow or Western diet for 4 months. (A) Fasting serum glucose and (B) fasting serum insulin were determined. (C) GTT. (D) ITT. (E,F) Hepatic mRNA expression in mice fasted overnight. Results are expressed as means and standard errors (n =6–12). \*Statistical significance ( $P < 0.05$ ) versus WT mice on a chow diet; \*\*statistically significant difference ( $P < 0.05$ ) versus HFD-fed WT mice. Abbreviations: GTT, glucose tolerance test; ITT, insulin tolerance test; Tg, transgenic; WT, wild-type.



**Fig. 6.**

Cyp7a1-tg mice showed increased hepatic glycogen storage. (A) Quantification of the hepatic glycogen content in overnight fasted female mice. (B) Female mice were fed chow or an HFD for 4 months. Hepatic glycogen was determined by PAS staining of liver sections from female mice fasted overnight. (C) Female mice on an HFD were fasted for 16 hours and refed for 6 hours. AKT was immunoprecipitated from pooled liver samples ( $n=6$ ); total and phosphorylated AKT was detected by WB. (D) Hepatic GSK3 $\beta$  and phosphorylated GSK3 $\beta$  were detected by WB in pooled liver samples ( $n=6$ ) from refed mice. Results are expressed as means and standard errors ( $n=6-8$ ). \*Statistical significance ( $P < 0.05$ ) versus WT mice on a chow diet; \*\*statistically significant difference ( $P < 0.05$ ) versus HFD-fed WT mice. Abbreviations: IP, immunoprecipitation; Tg, transgenic; WB, western blotting; WT, wild-type.

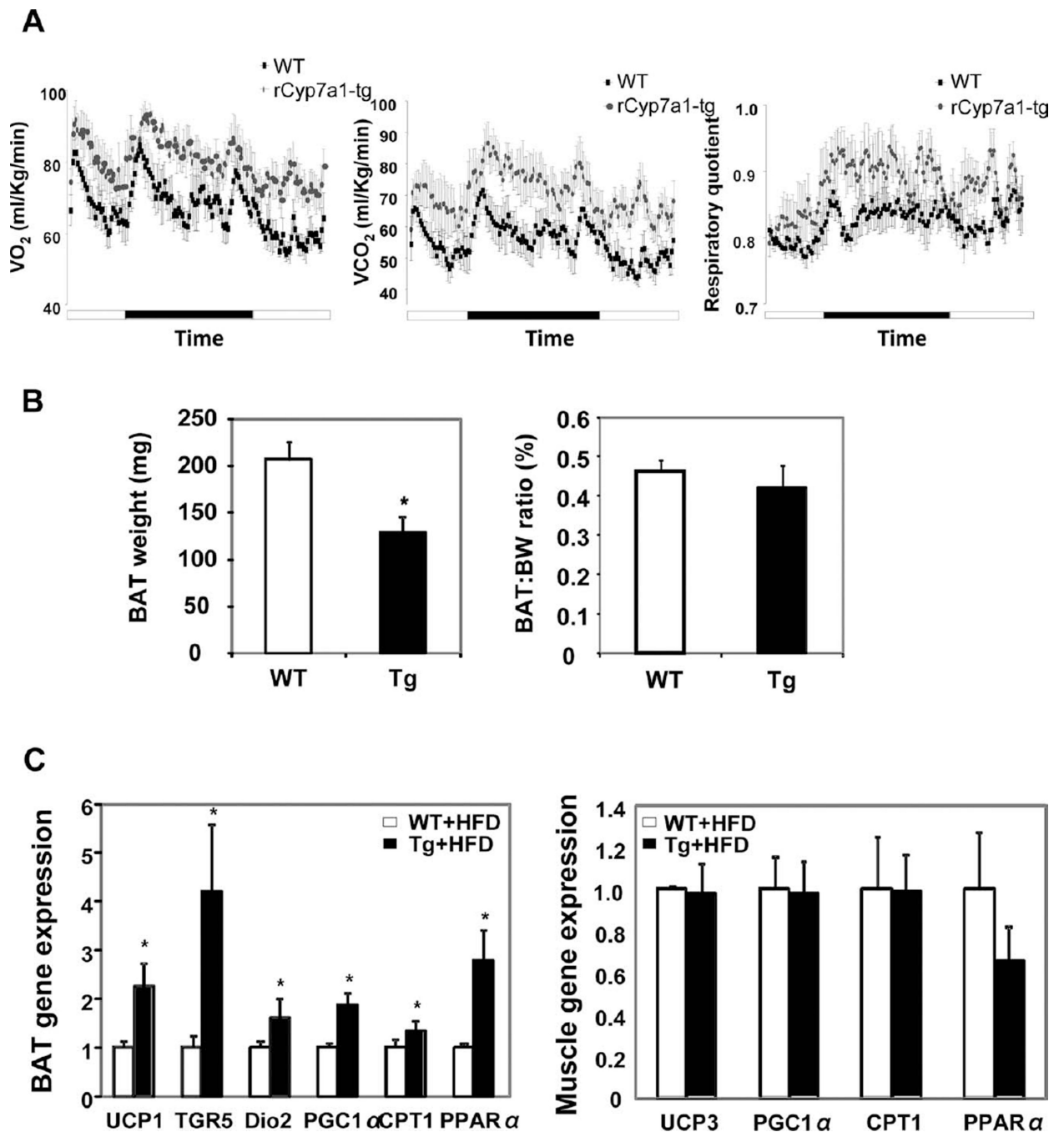


**Fig. 7.** Indirect calorimetry analysis of energy expenditure in Cyp7a1-tg mice. Female mice were fed either chow or an HFD for 2 months. (A) O<sub>2</sub> consumption and CO<sub>2</sub> production were determined in free-fed mice over a period of 24 hours by indirect calorimetry (n =4). For the time, a solid bar indicates the dark cycle, and an open bar indicates the light cycle. The left panel shows V<sub>O<sub>2</sub></sub>, the middle panel shows V<sub>CO<sub>2</sub></sub>, and the right panel shows RQ. (B) The brown adipose mass was determined in female mice fed an HFD (n =6). (C) Female mice on an HFD were refed for 6 hours after 16 hours of fasting, and mRNA expression was measured by real-time PCR (n = 6). Results are expressed as means and standard errors. \*Statistically significant difference ( $P < 0.05$ ) versus WT mice on an HFD. Abbreviations:

BW, body weight; CPT1, carnitine palmitoyltransferase 1; Dio2, type 2 deiodinase; PGC1 $\alpha$ , peroxisome proliferator-activated receptor  $\gamma$  coactivator-1 $\alpha$ ; PPAR $\alpha$ , peroxisome proliferator-activated receptor  $\alpha$ ; Tg, transgenic; WT, wild-type.

**Table 1**

## Hepatic mRNA Expression in WT and CYP7A1-tg Mice

	WT + Chow	Tg + Chow	WT + HFD	Tg + HFD
Fatty acid metabolism				
SREBP-1	1 ± 0.44	2.07 ± 0.16 <sup>*</sup>	10.46 ± 0.77 <sup>†</sup>	3.49 ± 0.62 <sup>*</sup>
SCD-1	1 ± 0.22	1.86 ± 0.5	18.45 ± 1.8 <sup>†</sup>	2.6 ± 0.63 <sup>*</sup>
FAS	1 ± 0.33	3 ± 0.3 <sup>*</sup>	0.8 ± 0.05	2.4 ± 0.5 <sup>*</sup>
ACC	1 ± 0.2	1.65 ± 0.23	1.24 ± 0.14	1.49 ± 0.22
CD36	1 ± 0.07	0.77 ± 0.08	1.65 ± 0.13 <sup>†</sup>	0.86 ± 0.15 <sup>*</sup>
Cholesterol metabolism				
HMG-CoA reductase	1 ± 0.53	11.18 ± 2.29 <sup>*</sup>	0.73 ± 0.06	19.6 ± 6.82 <sup>*</sup>
LDLR	1 ± 0.13	3.04 ± 0.4 <sup>*</sup>	1.27 ± 0.1	3 ± 0.55 <sup>*</sup>
SREBP-2	1 ± 0.2	2.48 ± 0.39 <sup>*</sup>	0.97 ± 0.07	2.79 ± 0.29 <sup>*</sup>
Bile acid metabolism				
mCYP7A1	1 ± 0.27	0.006 ± 0.003 <sup>*</sup>	2.28 ± 0.21 <sup>†</sup>	0.05 ± 0.03 <sup>*</sup>
mCYP8B1	1 ± 0.22	0.03 ± 0.01 <sup>*</sup>	0.29 ± 0.04 <sup>†</sup>	0.02 ± 0.008 <sup>*</sup>
SHP	1 ± 0.4	3.08 ± 0.9 <sup>*</sup>	0.92 ± 0.12	1.99 ± 0.4 <sup>*</sup>
rCyp7a1	ND	Ct = 19.4 ± 0.27	ND	Ct = 19.8 ± 0.29
Inflammatory cytokines				
TNFα	1 ± 0.1	1.37 ± 0.38	3.35 ± 0.39 <sup>†</sup>	1.6 ± 0.2 <sup>*</sup>
IL6	1 ± 0.09	0.94 ± 0.18	1.54 ± 0.24	0.73 ± 0.09 <sup>*</sup>
TGFβ1	1 ± 0.09	1.3 ± 0.3	2.47 ± 0.18 <sup>†</sup>	1.05 ± 0.07 <sup>*</sup>

Female mice were on chow or HFD for 4 months. The results are shown as means and standard errors (n = 6–10).

Abbreviations: ACC, acetyl coenzyme A carboxylase; CYP8B1, cholesterol 12α-hydroxylase; HMG-CoA, 3-hydroxy-3-methyl-glutaryl-coenzyme A; IL6, interleukin-6; LDLR, low-density lipoprotein receptor; ND, not determined; SCD-1, stearoyl-coenzyme A desaturase 1; Tg, transgenic; TGFβ1, transforming growth factor β1; TNFα, tumor necrosis factor α; WT, wild type.

<sup>\*</sup> Statistically significant difference ( $P < 0.05$ ) versus WT mice on the same diet.

<sup>†</sup> Statistically significant difference ( $P < 0.05$ ) versus WT mice on chow.